

# UNDERWATER IMAGE ENHANCEMENT TECHNIQUE BASED ON CYCLEGAN AND FREQUENCY DECOMPOSITION CORRECTION MODEL

LuHeng Wang, HaoLong Qi, LiYe Zhang\*

*School of Computer Science and Technology, Shandong University of Technology, Zibo 255000, Shandong, China.*

*Corresponding Author: LiYe Zhang, Email: zhangliye@sdut.edu.cn*

**Abstract:** Enhancing underwater images is a challenging task due to degradation from light scattering, absorption, and low contrast, which obscure important details. This paper proposes a novel method that combines Cycle-Consistent Generative Adversarial Network (CycleGAN) with Frequency Decomposition Correction to improve underwater image quality. Initially, CycleGAN was used to generate clearer images from blurred underwater photos, addressing distortions caused by the underwater environment. Next, Frequency Decomposition Correction separates the image into low-frequency (smooth areas) and high-frequency (details and edges) components. The low-frequency component is enhanced for better clarity, while the high-frequency component is sharpened to improve fine details and edges. The enhanced images are evaluated using PSNR, UCIQE, and UIQM metrics. Results show that CycleGAN significantly improves image quality, and the additional Frequency Decomposition Correction boosts clarity, contrast, and detail further. This combined method presents a promising solution for underwater image enhancement, with potential applications in marine research, underwater navigation, and environmental monitoring.

**Keywords:** CycleGAN; Frequency decomposition; Wavelet transform; CLAHE

## 1 INTRODUCTION

Underwater images are frequently degraded due to light scattering and absorption, leading to issues such as low contrast, color distortion, and blurriness [1]. These problems diminish visibility and complicate underwater analysis, making tasks like marine research, navigation, and environmental monitoring more challenging. The degradation results in distorted colors reduced clarity, and blurriness, which hampers important tasks like object detection and scene reconstruction in underwater environments [2]. Several techniques have been proposed to address these challenges in underwater image enhancement. One approach combines Contrast Limited Adaptive Histogram Equalization (CLAHE) with Total Generalized Variation (TGV) to improve contrast while preserving image details. Although this method improves UCIQE and PSNR metrics, it falls short in recovering color accuracy and fine details, especially in highly degraded images [3]. UIE-Net, a CNN-based approach, attempts to perform both color correction and haze removal. However, it struggles with artifacts and often fails to restore fine details in complex underwater conditions [4]. GAN-based methods like GAN-RS utilize multi-branch discriminators to preserve image content and remove noise. While they show effectiveness in real-time seabed experiments, these methods still do not adequately address the low contrast problem or recover fine details, which are essential for high-quality underwater image restoration [5]. UW-CycleGAN enhances unpaired underwater images by using content loss regularization and adversarial loss. Although it provides better visual quality, it does not fully address contrast enhancement or fine detail sharpening in severely distorted underwater conditions [6].

The paper addresses these limitations by proposing a novel method that combines CycleGAN with frequency-domain decomposition using wavelet transforms. Unlike existing approaches that enhance either color or details separately, the proposed method decomposes the image into low and high-frequency components [7]. CLAHE is applied to enhance the low-frequency components, improving overall clarity, while high-frequency sharpening is used to recover fine details [8]. This dual enhancement strategy not only enhances image contrast and clarity but also significantly improves detail preservation, overcoming the shortcomings of both traditional and GAN-based methods. The innovation of this paper lies in the integration of CycleGAN with frequency-domain correction, which allows for simultaneous enhancement of contrast and detail recovery. Experimental results demonstrate that the proposed method significantly improves image quality, as evaluated through PSNR, UCIQE, and UIQM metrics. By addressing the limitations of previous methods in recovering fine details and enhancing contrast, the paper presents a more effective and practical solution for underwater image enhancement, offering a robust approach to the challenges faced with underwater imaging.

## 2 MODEL

### 2.1 Cycle GAN model

#### 2.1.1 The structure of generator and discriminator

In CycleGAN, the generator transforms blurry underwater images (source domain) into clearer, enhanced images (target domain). Generator  $G$  produces enhanced images, while Generator  $F$  converts them back to their blurry versions. The generator utilizes a CNN with an encoder-decoder structure, where the encoder maps the input image to a latent space, and the decoder reconstructs it into the target domain.

The discriminator in CycleGAN differentiates between real and generated images. Discriminator  $D_X$  determines if an image belongs to the source domain (blurry underwater images) or is produced by Generator  $F$ , while Discriminator  $D_Y$  does the same for enhanced images generated by  $G$ . Both discriminators act as binary classifiers, aiming to reduce the likelihood of misclassifying generated images as real [9]. The generator and discriminator structures are illustrated in Figure 1:

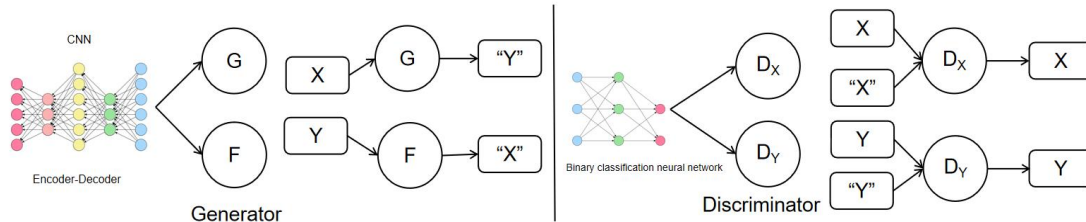


**Figure 1** The Structure of the Generator and the Discriminator

### 2.1.2 CycleGAN loss functions

#### 1. Cycle Consistency Loss and Identity Loss

The specific formula for this loss is as follows:

$$\mathcal{L}_{\text{cycle}}(G, F) = \left[ E_{x \sim P_{\text{data}}(x)} [\|F(G(x)) - x\|_1] + E_{y \sim P_{\text{data}}(y)} [\|G(F(y)) - y\|_1] \right]_{\min} \quad (1)$$

where  $E_{x \sim P_{\text{data}}(x)} [\|F(G(x)) - x\|_1]$ : This term calculates the difference between the source domain image  $x$  and the image  $F(G(x))$ , where  $G$  converts  $x$  to the target domain, and  $F$  maps it back to the source domain.  $E_{y \sim P_{\text{data}}(y)} [\|G(F(y)) - y\|_1]$ : This term calculates the difference between the target domain image  $y$  and the image  $G(F(y))$ , where  $F$  converts  $y$  to the source domain, and  $G$  transforms it back to the target domain. The goal is to minimize this difference, ensuring that the content of the original image  $y$  is preserved after the transformation [10].

The formula for identity loss is as follows:

$$\mathcal{L}_{\text{idt}}(G, F) = E_{y \sim P_{\text{data}}(y)} [\|G(y) - y\|_1] + E_{x \sim P_{\text{data}}(x)} [\|F(x) - x\|_1] \quad (2)$$

where  $E_{y \sim P_{\text{data}}(y)} [\|G(y) - y\|_1]$ : The term measures the difference between the target domain image  $y$  and the output generated by  $G$  when  $y$  is input into the generator.  $E_{x \sim P_{\text{data}}(x)} [\|F(x) - x\|_1]$ : The term calculates the difference between the source domain image  $x$  and the output generated by  $F$  when  $x$  is input into the generator [11].

#### 2. Total Loss Function and Training Process

The overall loss function combines adversarial loss, cycle consistency loss, and identity loss. Total Loss Function:

$$\mathcal{L}_{\text{CycleGAN}}(G, F, D_A, D_B) = \mathcal{L}_{\text{adv}}(G, D_Y) + \mathcal{L}_{\text{adv}}(F, D_X) + \lambda_1 \mathcal{L}_{\text{cycle}}(G, F) + \lambda_2 \mathcal{L}_{\text{idt}}(G, F) \quad (3)$$

where  $\lambda_1$  and  $\lambda_2$  are hyperparameters that control the relative contributions of the different loss terms. CycleGAN training includes Generator Training and Discriminator Training, which alternate optimization to gradually converge the model. Figure 2 shows the overall training process.

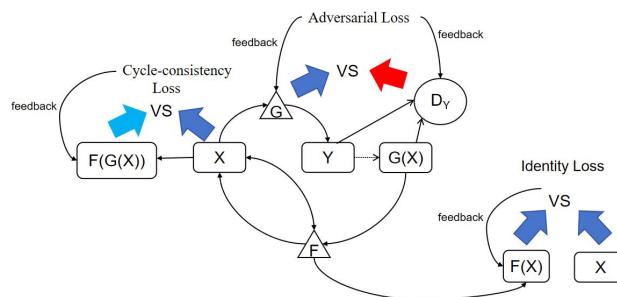


**Figure 2** Implementation Process of the Loss Function

CycleGAN training alternates between updating the generator and discriminator. The generator transforms a blurred image  $x$  into  $G(x)$  and a clear image  $y$  into  $F(y)$ . Adversarial loss ensures  $G(x)$  closely resembles  $y$ , deceiving discriminator  $D_Y$ , while cycle consistency loss ensures  $F(G(x)) \approx x$  and  $G(F(y)) \approx y$ . Identity loss minimizes changes to clear images fed into  $G$  and blurred images fed into  $F$ . The generator is trained to produce more realistic images. In discriminator training, real images  $y$  and generated images  $G(x)$  are used to calculate real and fake losses, refining the discriminator's ability to distinguish between them [12].

## 2.2 Frequency Decomposition Model

Frequency decomposition enhances images by separating them into low-frequency and high-frequency components. Wavelet Transform, a signal processing method, converts an image from the spatial domain to the frequency domain, with the low-frequency part capturing the main structure and the high-frequency part highlighting details like edges and textures [13]. Figure 3 shows its process.

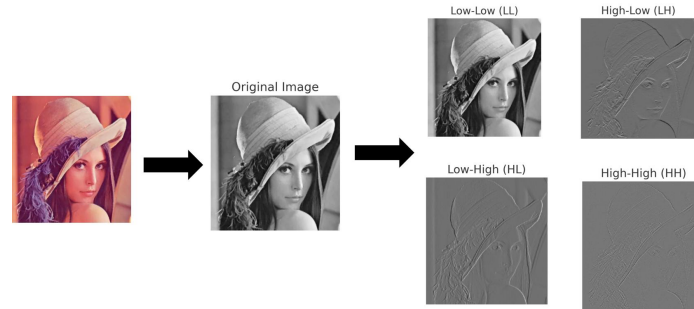


**Figure 3** The Process of Frequency Decomposition

The low-frequency part  $cA$  and high-frequency parts  $cH, cV, cD$  can be expressed by the wavelet transform as:

$$f(x, y) = cA + cH + cV + cD \quad (4)$$

where  $cA$  is the low-frequency part, and  $cH, cV, cD$  represent the horizontal, vertical, and diagonal detail coefficients, respectively.

The low-frequency component typically represents the general structure of an image. Since underwater images are often blurry due to light attenuation, enhancing the low-frequency component helps improve the overall clarity and brightness. Figure 4 demonstrates the effectiveness of the CLAHE algorithm.



**Figure 4** CLAHE Image

In this process, the low-frequency part is primarily enhanced by applying CLAHE to the image's luminance channel (L channel), further boosting the image's contrast. The CLAHE formula is:

$$CLAHE(I) = \frac{(I-\mu)}{\sigma} \cdot clip(I) + \mu \quad (5)$$

where  $I$  is the pixel value of the image,  $\mu$  is the local mean,  $\sigma$  is the local standard deviation, and  $clip()$  is the contrast limiting function.

The high-frequency part contains edges and details, which often become unclear in underwater images due to turbidity and light refraction. Sharpening the high-frequency components with filters like high-pass filters enhances image details and edges, improving clarity and realism.

In image synthesis, the low-frequency and high-frequency parts are enhanced separately and then combined with a specific weighting ratio to produce a balanced and realistic final image. The synthesis formula is as follows:

$$f_{enhanced}(x, y) = \alpha \cdot f_{low}(x, y) + \beta \cdot f_{high}(x, y) \quad (6)$$

### 2.3 Image Quality Indicators

To evaluate image quality, metrics like PSNR, UIQM, and UCIQE are commonly used.

PSNR measures the similarity between the original and enhanced images, with higher values indicating better image quality. It is calculated based on the mean squared error (MSE). The PSNR is defined as:

$$PSNR = 10 \cdot \log_{10} \left( \frac{(255)^2}{MSE} \right) \quad (7)$$

UCIQE evaluates image quality by focusing on color aspects such as saturation, contrast, and consistency, which influence perceived quality. It assesses the image using three parameters. The formula for UCIQE is as follows:

$$UCIQE = C_1 \cdot S_a + C_2 \cdot C_a + C_3 \cdot Q_a \quad (8)$$

$C_1=0.4680$   $C_2=0.2745$   $C_3=0.2576$  [14].

UIQM combines various quality metrics, including color contrast, consistency, saturation, and structural similarity index, to assess the perceptual quality of an image by considering both its color and structural elements. The formula for UIQM is as follows:

$$UIQM = C_1 \cdot C_b + C_2 \cdot Q_b + C_3 \cdot S_b \quad (9)$$

$C_1 = 0.2953$   $C_2 = 0.2953$   $C_3 = 0.1583$   $C_4 = 0.2471$  [15].

### 3 3 Result and Analyze

In this section, we evaluate the effectiveness of the underwater image enhancement method based on Cycle GAN and frequency decomposition correction.

#### 3.1 Training Part

##### 3.1.1 Dataset Description and preprocessing

In this experiment, this paper uses an underwater image dataset with clear images (target domain Y) and blurry images (source domain X), sourced from publicly available datasets covering environments like coral reefs and marine life. The images are preprocessed by standardizing their size to  $256 \times 256$  for CycleGAN training. Preprocessing steps include normalizing pixel values to the range  $[-1, 1]$  and applying data augmentation, such as random horizontal flipping, to improve model generalization.

##### 3.1.2 Weight setting of the loss function

Cycle Consistency Loss and Identity Loss are used to maintain image consistency and enhance model stability. The weights for each loss are shown in Table 1:

**Table 1** The Weights for Each Loss

Loss Type	Parameter	Value	Purpose
Cycle Consistency Loss	$\lambda_{\text{cycle}}$	10	Ensures the generator recovers the original input by transforming between domains.
Identity Loss	$\lambda_{\text{idt}}$	0.5	Maintains image identity, ensuring no drastic changes to target domain images

##### 3.1.3 Training strategy

During training, the generators G and F, along with discriminators  $D_Y$  and  $D_X$ , are alternately optimized to ensure stable learning. The learning rate begins at 0.0002 for the first 100 epochs and then decays linearly for the following 100 epochs to encourage stable convergence.

##### 3.1.4 Training results

To monitor the training process, this paper uses Visdom for real-time visualization, recording the changes in the model during the training process, in this case, domain A refers to the underwater blurry images, and domain B refers to the underwater clear images. Table 2 is an explanation of the coordinates in Figure 5 which shows the training iteration process:

**Table 2** Image Coordinate Interpretation

Name	Color	Description
cycle_A	green curve	The cycle consistency loss for underwater blurry images.
idt_A	red curve	The identity loss for underwater blurry images.

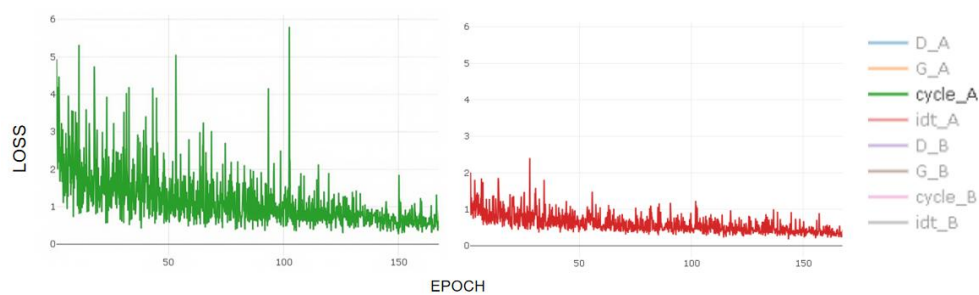


**Figure 5** Training Iteration Process

From the graph, it is evident that as training progresses, all losses stabilize, indicating that the generator and discriminator are progressively learning better generation and discrimination capabilities, and the stability of training is improving. Figure 6 shows these changes during training:



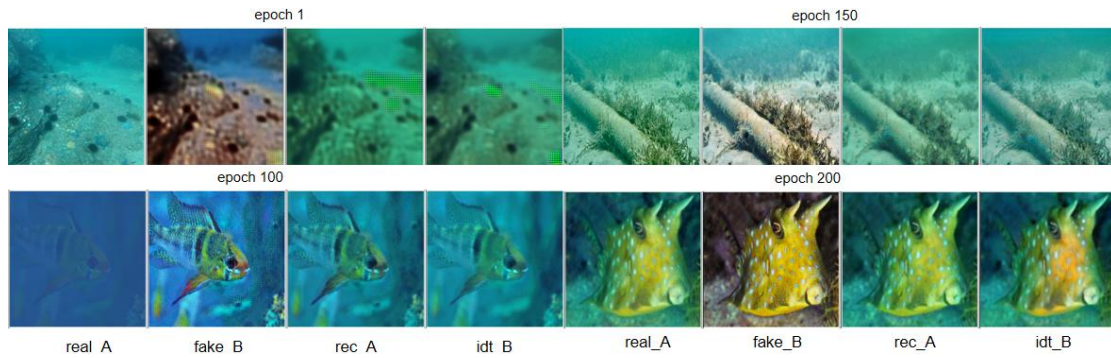


**Figure 6** Image Changes During Iteration

At Epoch 1, the generated underwater images are blurry with unrealistic colors. By Epoch 100, the images are sharper with more natural colors and enhanced details. By Epoch 150, the quality improves further with reduced noise and clearer contours. By Epoch 200, the generator consistently produces high-quality, realistic enhanced images. The experiment also shows that the training for both the cycle consistency loss function and the identity function gradually improves.

According to the content of the image, the four images correspond to the following parameters: *real\_A* is the real blurry underwater image, used as input. *fake\_B* is the generated clear image, produced by the generator. *rec\_A*: The underwater blurry image was restored by converting a generated clear image back to a blurry version. *idt\_B*: The identity function image, where a clear image is input into the generator and expected to remain unchanged.

As training progresses, CycleGAN improves its ability to transform blurry images into clearer ones, better matching the real underwater environment. By the end of training, the model weights reach an optimal state, ensuring stable and high-quality image generation.

### 3.2 Experimental Results

The article focuses on the bias in the convolutional neural network of the weight model, as shown in Figure 7:

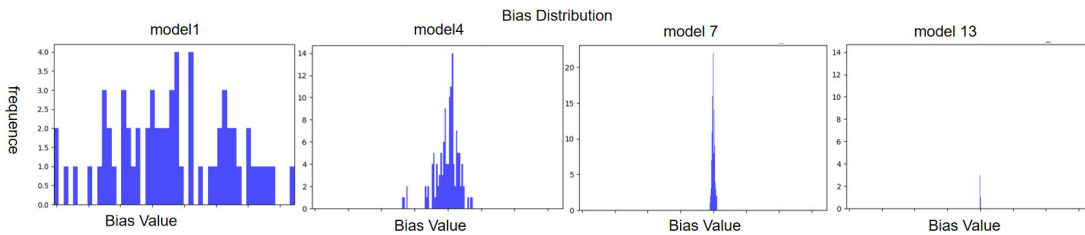


**Figure 7** Bias of Convolutional Neural Networks

As the depth of the convolutional network increases, the bias tends to stabilize, which indirectly proves the accuracy of the weight model.

The experiment involves loading the pre-trained generator (G) weights. During the training process, the generator G's weights are continuously optimized by minimizing the loss function of the Generative Adversarial Network (GAN). In this experiment, we loaded the generator weights saved during training and applied them to the underwater image enhancement task. The image processed by CycleGAN is shown in Figure 8:

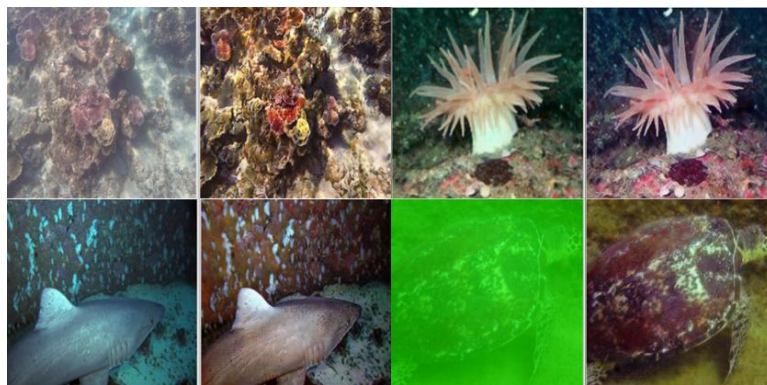


**Figure 8** Comparison of underwater enhancement effects

By loading the pre-trained generator weights, we successfully enhanced underwater blurry images, generating clear underwater images.

### 3.3 Frequency Decomposition Correction

After training the CycleGAN model, this paper enhanced the generated images using wavelet transform for frequency domain decomposition. The image is divided into four parts shown in Figure 9:

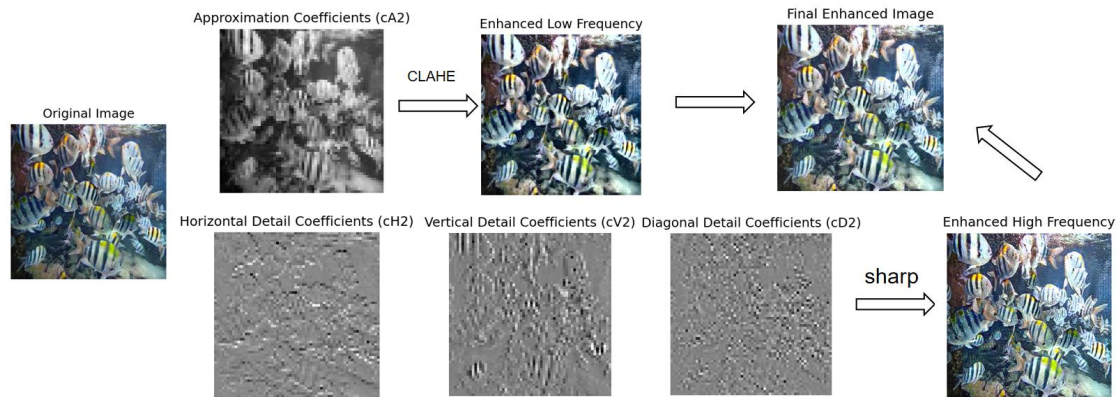


**Figure 9** Frequency Division Process

The enhanced low and high-frequency components are combined to produce the final image, improving its visual quality.

### 3.4 Analysis of experimental results

We conducted experiments comparing the image enhancement effects based on the frequency domain method and the frequency domain method after calibration. The experimental results are shown in Figure 10:

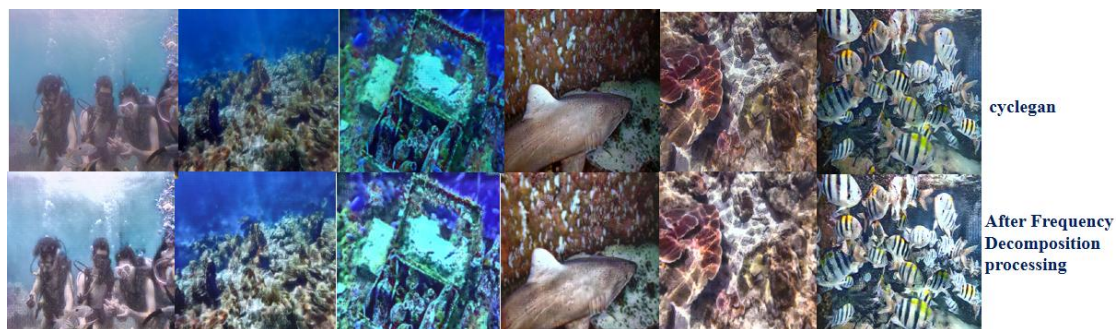


**Figure 10** Comparison of Frequency Division Processing Results

The following images show the original underwater image, the image enhanced using CycleGAN, and the image further enhanced using the frequency domain method. We can observe that the CycleGAN-enhanced image is clearer than the original image, while the image enhanced with the frequency domain method excels in sharpness and detail restoration. Figure 11 shows the difference between before and after image enhancement:

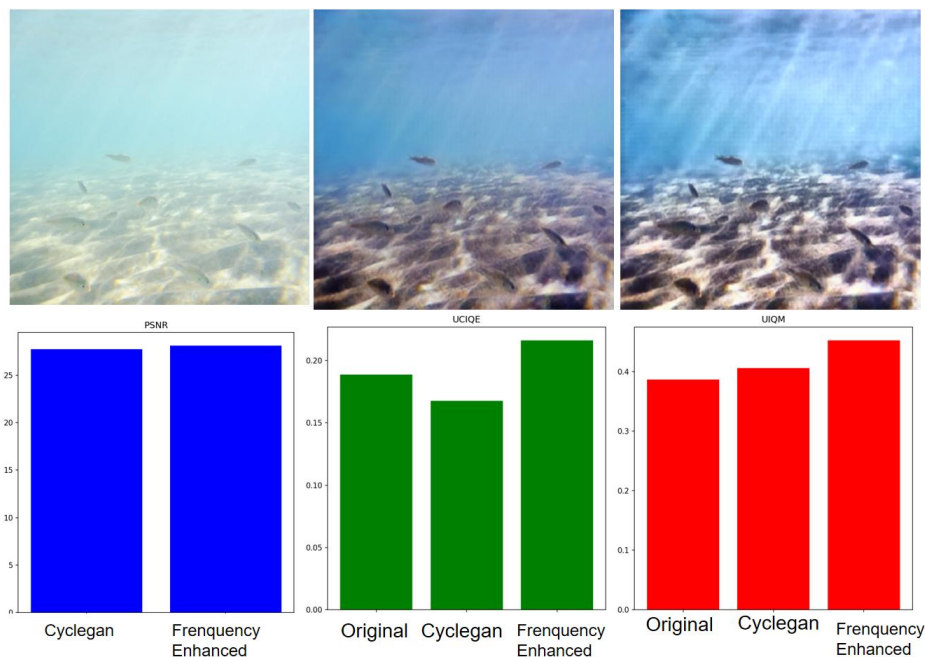


**Figure 11** Comparison of indicators

The following table 3 shows the average PSNR, UCIQE, and UIQM scores for the dataset images, including the original images, CycleGAN-enhanced images, and frequency division-enhanced images. The average score of datasets is shown in Table 3:

**Table 3** Average score of datasets

image type	PSNR (dB)	UCIQE	UIQM
original image		0.22	0.39
CycleGAN enhanced images	26.43	0.19	0.41
Frequency division method enhancement	28.75	0.24	0.43

PSNR shows that the frequency-enhanced image has a significant quality improvement, with a higher PSNR value, indicating that the enhanced image has less noise and better image quality. UCIQE decreases after CycleGAN processing, but the frequency method restores and further improves the UCIQE value of the image. UIQM shows that after the image is enhanced by CycleGAN, the value increases after correction with the frequency method. In the end, the image has significantly improved in clarity, details, and color.

#### 4 CONCLUSION

The article introduces a new underwater image enhancement method that combines CycleGAN with frequency-domain correction to improve clarity, contrast, and sharpness. Experimental results show that this method outperforms others in detail restoration and contrast enhancement. While CycleGAN alone enhances fine details, it reduces UCIQE values, affecting color consistency. By incorporating frequency-domain decomposition, the approach effectively addresses this issue. CLAHE enhances low-frequency components, improving image clarity, while high-frequency sharpening refines details, resulting in a more visually pleasing outcome. This combined method surpasses traditional pixel-to-pixel models in terms of generalization and robustness across various underwater conditions.

Future research will focus on optimizing wavelet transformations and exploring hybrid models to further enhance the robustness and efficiency of underwater image enhancement techniques.

#### COMPETING INTERESTS

The authors have no relevant financial or non-financial interests to disclose.

#### REFERENCES

- [1] Lepcha D C, Goyal B, Dogra A, et al. A deep journey into image enhancement: A survey of current and emerging trends. *Information Fusion*, 2023, 93:36-76.
- [2] Moghimi M K, Mohanna F. Real-time underwater image enhancement: a systematic review. *Journal of Real-Time Image Processing*, 2021, 18(5):1509-1525.

- [3] Kavitha S T, Vamsidhar A, Kumar S G, et al. Underwater Image Enhancement using Fusion of CLAHE and Total Generalized Variation. *Engineering Letters*, 2023, 31(4).
- [4] Wang Y, Zhang J, Cao Y, et al. A deep CNN method for underwater image enhancement. In: 2017 IEEE International Conference on Image Processing (ICIP). IEEE, 2017:1382-1386.
- [5] Chen X, Yu J, Kong S, et al. Towards real-time advancement of underwater visual quality with GAN. *IEEE Transactions on Industrial Electronics*, 2019, 66(12):9350-9359.
- [6] Du R, Li W, Chen S, Li C, Zhang Y. Unpaired Underwater Image Enhancement Based on CycleGAN. *Information*, 2022, 13:1.
- [7] Niu Yuzhen, Zhang Lingxin, Lan Jie, et al. Non-paired underwater image enhancement based on frequency division generative adversarial network. *Acta Sinica*, 2020, 1-18.
- [8] Shah R, Sheikh A, Shukla S, et al. Comparing effectiveness of gan and clahe for enhancing underwater images. In: 2023 7th International Conference on Trends in Electronics and Informatics (ICOEI). IEEE, 2023:1499-1503.
- [9] Goodfellow I, Pouget-Abadie J, Mirza M, et al. Generative adversarial nets. *Advances in Neural Information Processing Systems*, 2014, 27.
- [10] Wu J, Liu X, Lu Q, et al. FW-GAN: Underwater image enhancement using generative adversarial network with multi-scale fusion. *Signal Processing: Image Communication*, 2022, 109:116855.
- [11] Zhu J Y, Park T, Isola P, et al. Unpaired image-to-image translation using cycle-consistent adversarial networks. In: *Proceedings of the IEEE International Conference on Computer Vision*. 2017:2223-2232.
- [12] Du R, Li W, Chen S, et al. Unpaired underwater image enhancement based on CycleGAN. *Information*, 2021, 13(1):1.
- [13] Saifullah S, Suryotomo A P, Drezewski R, et al. Optimizing brain tumor segmentation through CNN U-Net with CLAHE-HE image enhancement. In: 2023 1st International Conference on Advanced Informatics and Intelligent Information Systems (ICAI3S 2023). Atlantis Press, 2024:90-101.
- [14] Kurinjimalar R, Pradeep J, Harikrishnan M. Underwater Image Enhancement Using Gaussian Pyramid, Laplacian Pyramid and Contrast Limited Adaptive Histogram Equalization. In: 2024 IEEE 3rd World Conference on Applied Intelligence and Computing (AIC). IEEE, 2024:729-734.
- [15] Tang X, Wu Y. Single Underwater Image Enhancement Based on Transmission Map Weighted Fusion and Adaptive Color Correction. In: 2023 International Conference on Image Processing, Computer Vision and Machine Learning (ICICML). IEEE, 2023:25-28.